




Detection of Barrett's neoplasia with a near-infrared fluorescent heterodimeric peptide



Authors

Jing Chen¹ , Yang Jiang², Tse-Shao Chang³ , Joel H. Rubenstein¹, Richard S. Kwon¹, Erik J. Wamsteker¹, Anoop Prabhu¹, Lili Zhao⁴, Henry D. Appelman⁵, Scott R. Owens⁵, David G. Beer⁶, D. Kim Turgeon¹, Eric J. Seibel⁷, Thomas D. Wang^{1,3,8} 

Institutions

- 1 Division of Gastroenterology, Department of Internal Medicine, University of Michigan, Ann Arbor, Michigan, USA
- 2 Department of Bioengineering, University of Washington, Seattle, Washington, USA
- 3 Department of Mechanical Engineering, University of Michigan, Ann Arbor, Michigan, USA
- 4 Department of Biostatistics, University of Michigan, Ann Arbor, Michigan, USA
- 5 Department of Pathology, University of Michigan, Ann Arbor, Michigan, USA
- 6 Department of Surgery, Section of Thoracic Surgery, University of Michigan, Ann Arbor, Michigan, USA
- 7 Department of Mechanical Engineering, University of Washington, Seattle, Washington, USA
- 8 Department of Biomedical Engineering, University of Michigan, Ann Arbor, Michigan, USA

submitted 1.9.2021

accepted after revision 4.3.2022

published online 17.3.2022

 Supplementary material

Supplementary material is available under

<https://doi.org/10.1055/a-1801-2406>

Bibliography

Endoscopy 2022; 54: 1198–1204

DOI 10.1055/a-1801-2406

ISSN 0013-726X

© 2022. The Author(s).

This is an open access article published by Thieme under the terms of the Creative Commons Attribution-NonDerivative-NonCommercial License, permitting copying and reproduction so long as the original work is given appropriate credit. Contents may not be used for commercial purposes, or adapted, remixed, transformed or built upon. (<https://creativecommons.org/licenses/by-nc-nd/4.0/>)

Georg Thieme Verlag KG, Rüdigerstraße 14,
70469 Stuttgart, Germany

Corresponding author

Thomas D. Wang, MD, PhD, Departments of Medicine, Biomedical Engineering, and Mechanical Engineering, Division of Gastroenterology, University of Michigan, 109 Zina Pitcher Pl. BSRB 1522, Ann Arbor, MI 48109-2200, USA
thomaswa@umich.edu

ABSTRACT

Background Esophageal adenocarcinoma (EAC) is a molecularly heterogeneous disease with poor prognosis that is rising rapidly in incidence. We aimed to demonstrate specific binding by a peptide heterodimer to Barrett's neoplasia in human subjects.

Methods Peptide monomers specific for EGFR and ErbB2 were arranged in a heterodimer configuration and labeled with IRDye800. This near-infrared (NIR) contrast agent was topically administered to patients with Barrett's esophagus (BE) undergoing either endoscopic therapy or surveillance. Fluorescence images were collected using a flexible fiber accessory passed through the instrument channel of an upper gastrointestinal endoscope. Fluorescence images were collected from 31 BE patients. A deep learning model was used to segment the target (T) and background (B) regions.

Results The mean target-to-background (T/B) ratio was significantly greater for high grade dysplasia (HGD) and EAC versus BE, low grade dysplasia (LGD), and squamous epithelium. At a T/B ratio of 1.5, sensitivity and specificity of 94.1 % and 92.6 %, respectively, were achieved for the detection of Barrett's neoplasia with an area under the curve of 0.95. No adverse events attributed to the heterodimer were found. EGFR and ErbB2 expression were validated in the resected specimens.

Conclusions This "first-in-human" clinical study demonstrates the feasibility of detection of early Barrett's neoplasia using a NIR-labeled peptide heterodimer.

Introduction

Esophageal adenocarcinoma (EAC) has been rising rapidly in incidence in Western countries, and is associated with a low 5-year survival rate of ~20% [1, 2]. Improved methods for early cancer detection are needed to mitigate this growing health-care burden. Barrett's esophagus (BE) is a precursor condition that progresses to EAC via low grade dysplasia (LGD) and high grade dysplasia (HGD) [3]. The effectiveness of endoscopic screening with white-light illumination and random biopsy is limited by sampling error [4]. Regions of dysplasia are often characterized by a flat architecture and patchy distribution [5]. Therefore, wide-field endoscopic imaging technologies that target molecular expression may improve diagnostic performance [6].

During progression of BE to EAC, the epithelium undergoes a number of molecular changes that may be detected by targeted imaging methods. EGFR and ErbB2 are cell surface targets that have been found to be gene amplified and highly overexpressed in surgically resected specimens of HGD and EAC [7, 8]. We have previously identified and validated 7mer peptides specific for EGFR and ErbB2 [9, 10], and have arranged these monomers in a heterodimer configuration [11, 12]. Improved imaging performance was demonstrated in a preclinical model of EAC. This heterobivalent peptide was labeled with IR-Dye800, a near-infrared (NIR) fluorophore, to provide high contrast. In this study, we aimed to clinically translate this NIR-labeled heterodimer by performing a "first-in-human" clinical study to demonstrate its feasibility for the early detection of Barrett's neoplasia.

Methods

NIR fluorescently labeled peptide heterodimer

IRDye800CW maleimide (LI-COR) was conjugated to the free sulfhydryl (-SH) on the terminal cysteine of the peptide heterodimer. The NIR-labeled heterodimer was synthesized using current good manufacturing practices (cGMP) methods by CPC Scientific (Table 1 s, see online-only Supplementary Material) and was lyophilized and aliquoted in sterile 10-mL amber vials (protection from light) in quantities of 0.6 and 1.8 mg. Purity $\geq 95.0\%$ was measured by high performance liquid chromatography (HPLC), and a mass-to-charge (m/z) ratio of 3510.06 was found using electrospray ionization (ESI) mass spectroscopy. Stability of the lyophilized heterodimer was monitored by appearance, purity, and molecular weight every 6 months over the duration of the study (Table 2 s). Patient use of the heterodimer was regulated under IND #139,834.

In vivo imaging

Consecutive patients referred to Michigan Medicine for either evaluation or therapy of Barrett's neoplasia were recruited. Inclusion criteria included: (i) history of Barrett's neoplasia; (ii) medically able to tolerate upper gastrointestinal (GI) endoscopy; and (iii) age over 18. Exclusion criteria included: (i) history of esophagectomy and (ii) on an active chemotherapy or radiation protocol. Prior endoscopic therapy was not an exclusion.

The clinical study was approved by the Michigan Medicine institutional review board (IRB). The lyophilized peptide heterodimer was reconstituted in 5 mL of normal saline, and the solution was topically administered to the distal esophagus using a standard spray catheter (PW-5V-1; Olympus). The flexible fiber imaging instrument was passed through the working channel of the endoscope to collect in vivo images. The fluorescence images were evaluated using a deep learning algorithm to quantify the T/B ratios (see Appendix 1 s). Tissue specimens were collected with either standard pinch biopsy forceps or using endoscopic mucosal resection (EMR) from regions that appeared suspicious on imaging.

Histology

All specimens were processed for routine histology, and were evaluated by an expert GI pathologist (H.D.A.) without knowledge of the patient's clinical information or the in vivo imaging results. Immunohistochemistry was performed using a standard protocol, as described previously [9, 10]. Monoclonal antibodies used include anti-EGFR (H11; mouse monoclonal antibody #MA-13070, Invitrogen) and anti-ErbB2 (#29D8; rabbit monoclonal antibody #2165, Cell Signaling Inc). Immunohistochemistry scoring was performed independently by a second expert GI pathologist (S.R.O.). Scoring was performed using the DAKO HercepTest guidelines.

Results

NIR fluorescently labeled peptide heterodimer

The monomer peptides QRHKPRE and KSPNPRF, specific for EGFR and ErbB2, respectively, were connected by a short triethyleneglycol linker (E3) to the α -, ξ - amino groups of lysine to form the heterodimeric structure. IRDye800 was attached to the terminal cysteine of the heterodimer via thiol-ene click chemistry, hereafter called QRH*-KSP*-E3-IRDye800 (Fig. 1 s, part A). The absorbance and emission spectra of the heterodimer had minimal overlap with standard white-light illumination (400–700 nm; Fig. 1 s, part B). QRH*-KSP*-E3-IRDye800 was synthesized in compliance with cGMP (Table 1 s). Purity $\geq 95.0\%$ was measured by HPLC (Fig. 2 s, part A), and a mass-to-charge (m/z) ratio of 3510.06 was found using ESI mass spectra (Fig. 2 s, part B).

Patient demographics

A clinical imaging study was performed to evaluate the detection of early Barrett's neoplasia using the heterodimer in 31 patients with a history of Barrett's neoplasia (► **Table 1**). The mean (SD) age of the patients was 62.1 (13.0) years and their mean (SD) body mass index (BMI) was 34.4 (10.7) kg/m². A total of 11, 3, 4, and 13 patients with non-dysplastic BE, LGD, HGD, and EAC, respectively, confirmed by histopathology, were enrolled.

Imaging instrument

A flexible fiber multimodal scanning fiber endoscope was passed through the instrument channel of a standard upper GI endoscope to collect wide-field images in vivo [13] (Fig. 3 s,

► Table 1 Demographics of the 31 patients with Barrett's esophagus who had near-infrared fluorescence images collected in vivo from the distal esophagus following administration of QRH*-KSP*-IRDye800.

| Patient number | Age, years | Sex | BMI, kg/m ² | Prague criteria ¹ (stage) | Tissue sampling ² | Pathology ³ |
|----------------|------------|--------|------------------------|--------------------------------------|------------------------------|------------------------|
| 1 | 61 | Male | 31.6 | C10M10 | EMR/biopsy | NDBE |
| 2 | 83 | Male | 35.2 | C0M1 | Biopsy | NDBE |
| 3 | 64 | Male | 32.7 | C2M3 | Biopsy | NDBE |
| 4 | 54 | Male | 51.9 | C2M7 | EMR/biopsy | NDBE |
| 5 | 62 | Male | 24.8 | C10M10 | Biopsy | NDBE |
| 6 | 64 | Male | 27.4 | C0M0I2 | Biopsy | NDBE |
| 7 | 52 | Male | 31.4 | C0M0.5 | EMR/biopsy | NDBE |
| 8 | 44 | Male | 41.7 | C0M0.5I1 | Biopsy | NDBE |
| 9 | 77 | Male | 31.1 | C0M2I4 | Biopsy | NDBE |
| 10 | 76 | Male | 33.2 | C0M0.5 | Biopsy | NDBE |
| 11 | 80 | Male | 39.2 | C9M9 | EMR/biopsy | NDBE |
| 12 | 62 | Female | 21.6 | C0M8I13 | Biopsy | LGD |
| 13 | 51 | Male | 32.4 | C10M12 | Biopsy | LGD |
| 14 | 64 | Female | 31.8 | C1M6 | Biopsy | LGD |
| 15 | 63 | Male | 30.4 | C0M1 | EMR/biopsy | HGD |
| 16 | 61 | Male | 23.6 | C4M6 | Biopsy | HGD |
| 17 | 30 | Male | 28.7 | C1M4 | EMR | HGD |
| 18 | 55 | Male | 42.6 | C0M3 | EMR/biopsy | HGD |
| 19 | 81 | Female | 24.1 | C0M1(T1a) | EMR/biopsy | EAC |
| 20 | 57 | Male | 39.3 | C0M1 | Biopsy | EAC |
| 21 | 84 | Male | 25.9 | C6M7 | Biopsy | EAC |
| 22 | 79 | Female | 20.8 | T3N1 | Biopsy | EAC |
| 23 | 54 | Male | 51.9 | C2M7(T1a) | EMR | EAC |
| 24 | 46 | Male | 47.1 | C6M7 | EMR/biopsy | EAC |
| 25 | 72 | Male | 31.6 | C0M0.5 | EMR | EAC |
| 26 | 59 | Male | 45.9 | C0M2 | EMR | EAC |
| 27 | 46 | Male | 52.4 | C4M4 | EMR/biopsy | EAC |
| 28 | 52 | Female | 38.9 | T1a | EMR/biopsy | EAC |
| 29 | 52 | Male | 21.1 | C0M3 | EMR | EAC |
| 30 | 66 | Male | 33.1 | C8M10 | EMR/biopsy | EAC |
| 31 | 74 | Male | 30.5 | C1M1 | EMR/biopsy | EAC |

BMI, body mass index; EMR, endoscopic mucosal resection; NDBE, non-dysplastic Barrett's esophagus; LGD, low grade dysplasia; HGD, high grade dysplasia; EAC, esophageal adenocarcinoma

¹ Modified Prague criteria (C, circumferential; M, maximum; I, island) were used to define the anatomic extent of the Barrett's segment based on conventional white-light endoscopy.

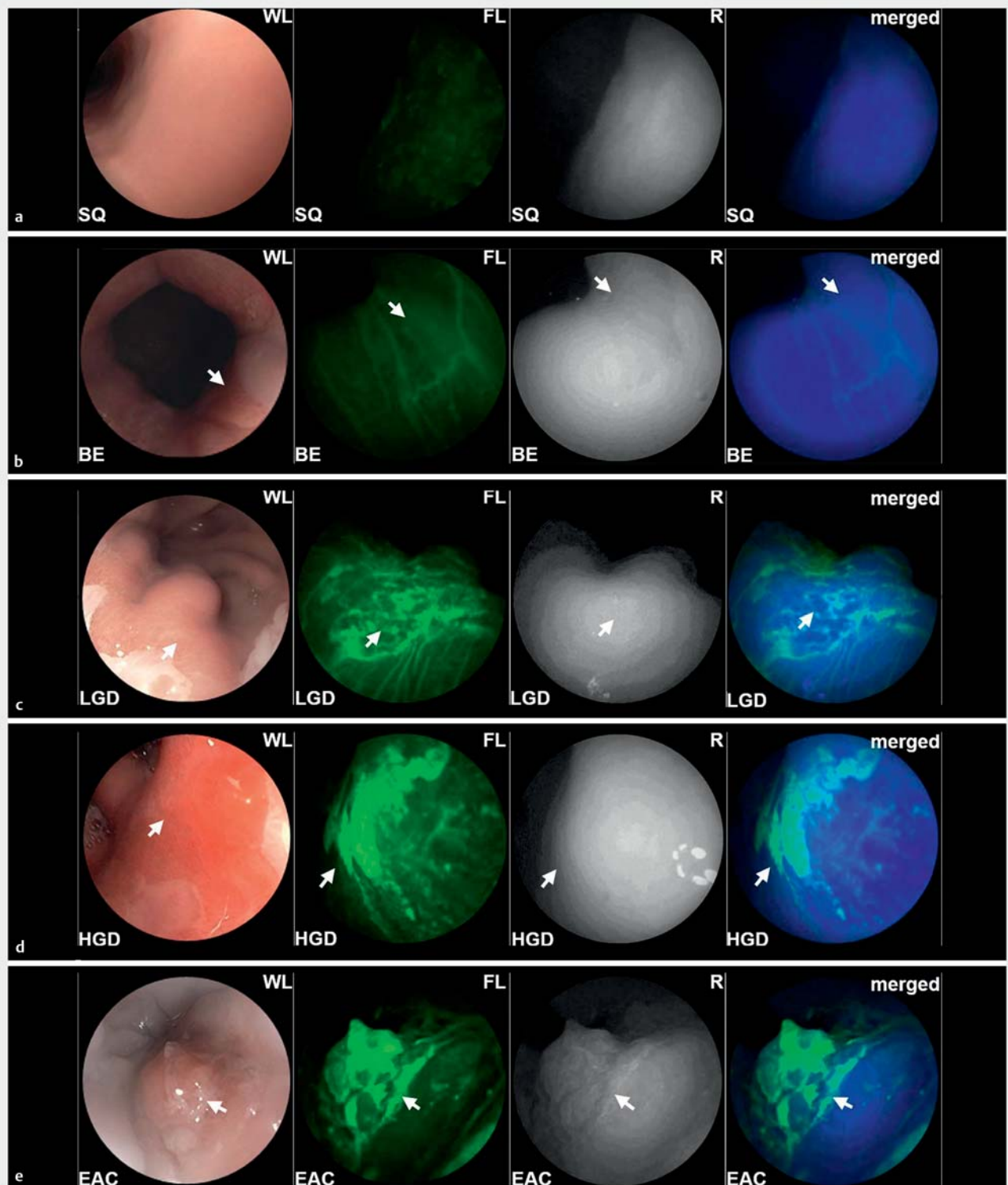
² Tissue sampling was performed by either EMR or standard pinch biopsy.

³ Pathology represents the highest grade found.

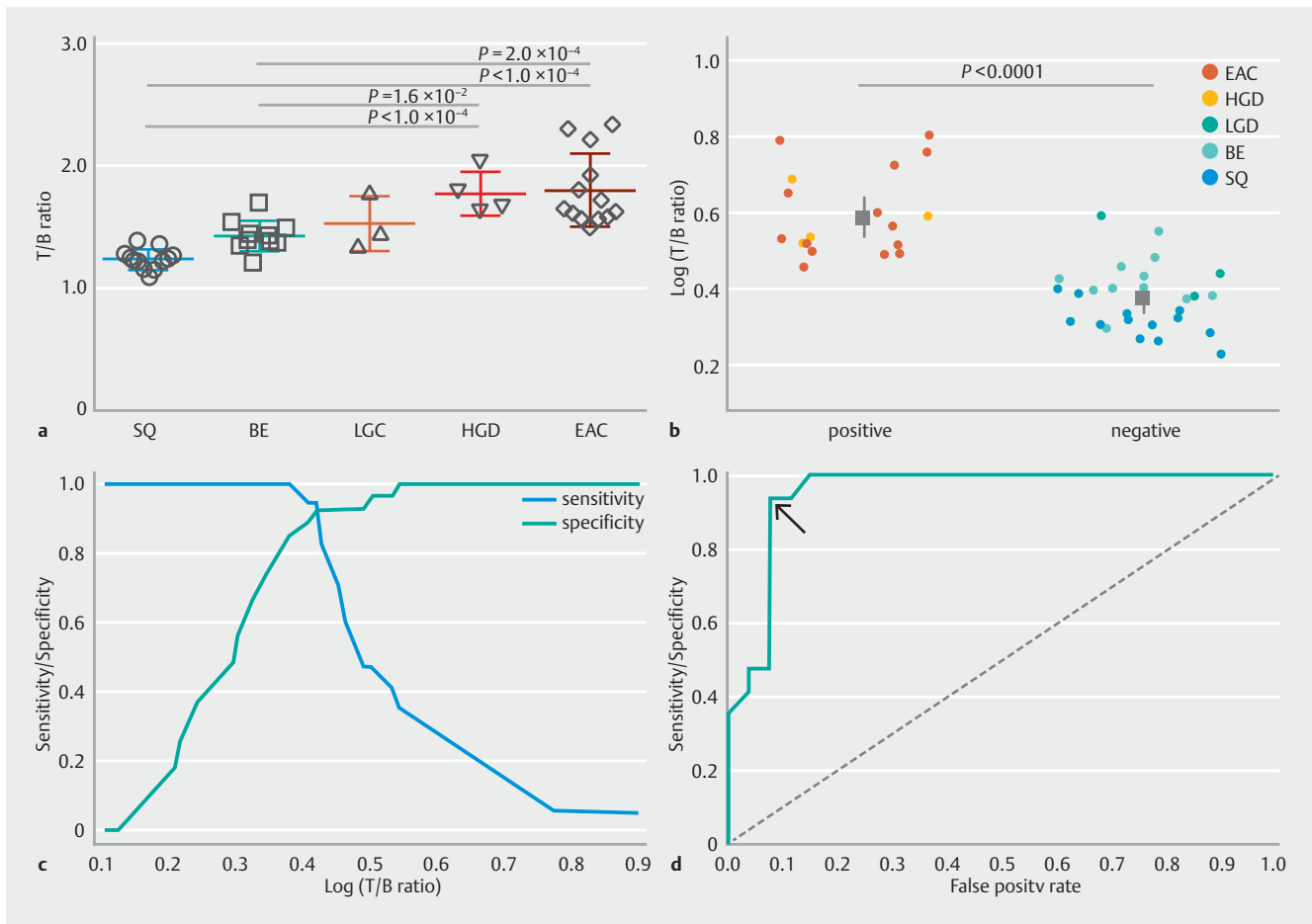
part A). Excitation at λ_{ex} 785 nm was delivered via a scanning fiber. Fluorescence and reflectance were collected by a ring of multimode fibers at 30 frames per second, and separated for detection (Fig. 3 s, part B).

Imaging study in vivo

On the fluorescence images, minimal background was seen from areas of esophagus prior to peptide administration (► **Video 1**). The mean duration for image capture was ~7 minutes



► **Fig. 1** Representative in vivo images using white light (WL), fluorescence (FL), and reflectance (R) collected endoscopically following topical administration of QRH*-KSP*-IRDye800 onto: **a** squamous epithelium (SQ); **b** non-dysplastic Barrett's esophagus (BE); **c** low grade dysplasia (LGD); **d** high grade dysplasia (HGD); **e** esophageal adenocarcinoma (EAC). In the white-light images, the salmon-red areas (arrows) identify regions of BE. Co-registered reflectance images provide anatomical correlation. The merged images show areas of high contrast in pseudocolor that indicate regions of increased target expression (arrows).



► Fig. 2 The imaging performance shown graphically. **a** A scatter plot of the T/B ratios measured from the near-infrared fluorescence images illustrate the mean (SD) values for squamous epithelium (SQ; n = 13), Barrett’s esophagus (BE; n = 11), low grade dysplasia (LGD; n = 3), high grade dysplasia (HGD; n = 4), and esophageal adenocarcinoma (EAC; n = 13), which were found to be 1.24 (0.06), 1.40 (0.10), 1.49 (0.19), 1.69 (0.15), and 1.72 (0.24), respectively (the results were confirmed by histology using H&E staining and P values were determined using a Tukey–Kramer test). **b** Log-transformed data were classified as either positive (HGD, EAC) or negative (SQ, BE, LGD) for Barrett’s neoplasia; mean (SD) T/B ratios of 1.71 (0.22) and 1.33 (0.13), respectively, were measured ($P < 0.001$). **c** The tradeoffs in imaging performance. **d** Receiver operating characteristic (ROC) curves showing the optimal values of 94.1% sensitivity and 92.6% specificity (arrow). AUC, area under the curve.

(range 3–15 minutes). Representative high definition white-light, fluorescence, and reflectance images are shown for squamous, non-dysplastic BE, and LGD (► Fig. 1a–c). The location of BE in the white-light images is defined by mucosa with a salmon-pink appearance located above the gastric folds. The border between squamous epithelium and BE can be clearly distinguished on fluorescence. Representative in vivo images showing increased fluorescence intensities from regions of HGD and EAC are shown in ► Fig. 1d,e.

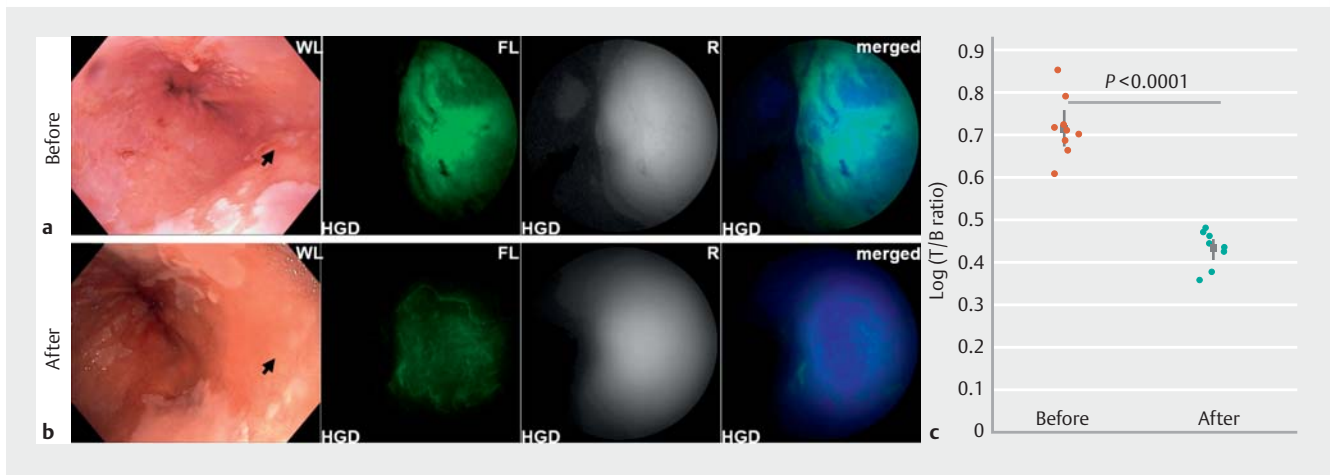
Image analysis

Fluorescence images collected from a total of 31 patients were evaluated. A deep learning model was used to segment the target (T) and background (B) to calculate the T/B ratio. This parameter was calculated at ~15 frames per second. The T/B ratios measured for squamous epithelium, BE, LGD, HGD, and EAC are shown (► Fig. 2a). The mean values for HGD and EAC were significantly greater than that for BE. The data were sep-

arated as either positive (HGD, EAC) or negative (squamous epithelium, BE, LGD) for either neoplasia or high risk Barrett’s, and the mean T/B ratio for positive was found to be significantly greater than for negative (► Fig. 2b). Tradeoffs in imaging performance are shown (► Fig. 2c). At a T/B ratio of 1.5, the receiver operating characteristic (ROC) curve showed 94.1% sensitivity and 92.6% specificity with an area under the curve of 0.95 for the detection of either HGD or EAC (► Fig. 2d). At this threshold, the imaging results revealed 16, 1, 25, and 2 true positives, false positives, true negatives, and false negatives, respectively.

Image-guided therapy

The potential for this technique to guide therapy of HGD or neoplasia was demonstrated in a patient with HGD where fluorescence images were collected from the same location in the distal esophagus before and 14 weeks after endoscopic resection (► Fig. 3a,b). The image intensities were quantified and



► **Fig. 3** A set of white light (WL), near-infrared fluorescence (FL), and reflectance (R) images from a patient with high grade dysplasia: **a** before treatment; and **b** 14 weeks after endoscopic mucosal resection. Prior to resection, the WL images show a Barrett's esophagus segment with a region of high grade dysplasia (arrow), which shows greater intensity on the FL images. **c** Log T/B ratios before and after therapy show mean (SD) results of 1.72 (0.13) vs. 1.39 (0.05) respectively; $P < 0.001$ by paired, one-tailed *t* test.

the mean T/B ratio was found to be significantly greater before therapy ► **Fig. 3c**).

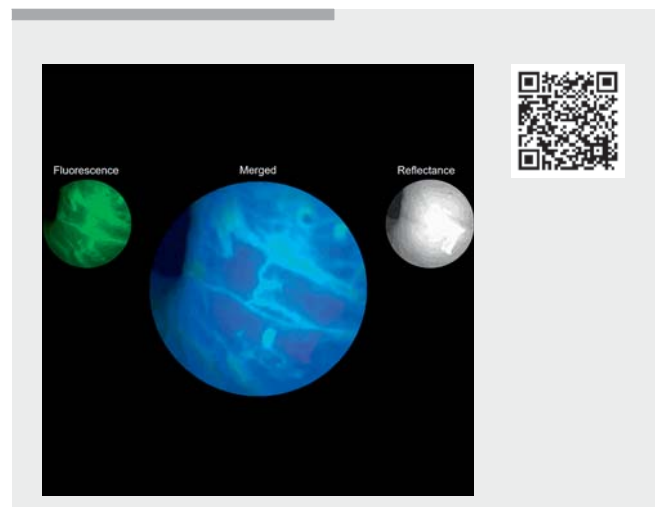
Histology

The presence of Barrett's neoplasia was validated by pathological assessment of routine histology. The pathology was defined by the highest grade found. Immunohistochemistry was used to validate EGFR and ErbB2 expression in the resected specimens. Minimal expression of either EGFR or ErbB2 was observed in squamous epithelium, BE, and LGD, while significantly higher expression was seen in HGD and EAC (Fig. 4s).

Discussion

Targeted wide-field fluorescence imaging is a promising approach for early cancer detection in patients with BE during endoscopy. Barrett's neoplasia is molecularly heterogeneous, and target expression levels can vary widely among different patients and even within the same esophagus, therefore concurrent imaging of multiple targets may improve diagnostic performance. Previously, lectins have been investigated for the detection of Barrett's neoplasia ex vivo [14], but have not been demonstrated clinically. Bevacizumab, an FDA-approved therapeutic antibody originally developed for anti-angiogenesis, was repurposed for diagnostic imaging by labeling with IRDye800 [15]. Advanced endoscopy techniques, such as chromoendoscopy, narrow-band imaging, and autofluorescence imaging, have been evaluated clinically, but provide intrinsically low contrast and are based on non-specific mechanisms. We developed monomer peptides specific for either EGFR and ErbB2 [8, 9] to detect HGD or EAC in a previous clinical study in which the two peptides were topically administered separately [13]. Here, we arranged the monomer peptides in a heterobivalent configuration. This structure was achieved by matching the linker length with the mean distance between the extracellular binding domains of each target.

Heterodimers are playing an emerging role in molecular imaging for their ability to visualize multiple targets currently [16–20]. The integration of two unique ligands into a single entity that recognizes different targets can enhance binding effects and improve diagnostic performance. High sensitivity can be achieved by simultaneous detection of two unique targets, and greater specificity may arise from the structure binding to a larger combined region of the target epitope by comparison with the monomers. These advantages can potentially detect molecular targets at lower levels of expression and may be useful for identifying EAC at an earlier timepoint or in the



► **Video 1** Imaging studies with white light, fluorescence, reflectance, and merged images using the near-infrared (NIR)-labeled heterodimer and a multimodal scanning fiber endoscope are shown for patients with esophageal adenocarcinoma, high and low grade dysplasia, Barrett's esophagus, and squamous epithelium.

Online content viewable at:
<https://doi.org/10.1055/a-1801-2406>

pre-malignant stage. Moreover, this integrated imaging agent simplifies the clinical procedure whereby only one rather than two imaging agents are administered during endoscopy. Previously, the apparent dissociation constant (binding affinity) of the heterodimer was found to increase by between 2- to 4-fold versus either monomer alone, while the apparent association time constant (binding onset) of $k=4.5$ minutes was found to be similar [10]. After the peptides were administered, a complete endoscopic examination of the upper digestive tract was performed prior to imaging.

The fluorescence emission spectrum of IRDye800 has minimal overlap with that of standard white-light illumination. Use of this fluorophore allows the physician to visualize anatomical features on the white-light image and molecular expression on the fluorescence image at the same time. Topical administration of this imaging agent was found to be safe in human subjects. A limitation of this study is that fluorescence images were collected from only a small number of patients. A randomized controlled study with a larger number of patients is needed to more definitively characterize imaging performance.

Herein, we have demonstrated the clinical use of two unique 7mer peptides specific for either EGFR or ErbB2 arranged in a heterodimer configuration to detect either HGD or EAC. The use of targeted imaging methodologies may help clarify the pathological classification of Barrett's mucosa by providing molecular expression levels and patterns. This study represents the first use of a heterobivalent peptide in human subjects combined with wide-field fluorescence imaging. This integrated imaging methodology has the potential to improve visualization of flat and subtle pre-malignant lesions in BE patients who are at increased risk for cancer.

Acknowledgments

We thank E. Brady, A. Cawthon, and C. Nolan for clinical support, and B.R. Reisdorph for regulatory support.

Competing interests

J. Chen and T.D. Wang are inventors on patents filed by the University of Michigan on the peptide heterodimer used in the study. E.J. Seibel is an inventor on patents filed by the University of Washington on the multimodal scanning fiber endoscope. The remaining authors declare that they have no conflict of interest.

Funding

National Institutes of Health CA163059

Clinical trial

Trial Registration: ClinicalTrials.gov | Registration number (trial ID): NCT03852576 | Type of study: randomized

References

- [1] Siegel RL, Miller KD, Jemal A. Cancer statistics 2020. *CA Cancer J Clin* 2020; 70: 7–30
- [2] He H, Chen N, Hou Y et al. Trends in the incidence and survival of patients with esophageal cancer: A SEER database analysis. *Thorac Cancer* 2020; 11: 1121–1128
- [3] Prasad GA, Bansal A, Sharma P et al. Predictors of progression in Barrett's esophagus: current knowledge and future directions. *Am J Gastroenterol* 2010; 105: 1490–1502
- [4] Sharma P, Savides TJ, Canto MI et al. The American Society for Gastrointestinal Endoscopy PIVI (Preservation and Incorporation of Valuable Endoscopic Innovations) on imaging in Barrett's Esophagus. *Gastrointest Endosc* 2012; 76: 252–254
- [5] Spechler SJ, Sharma P. American Gastroenterological Association. et al. American Gastroenterological Association medical position statement on the management of Barrett's esophagus. *Gastroenterology* 2011; 140: 1084–1091
- [6] Sturm MB, Wang TD. Endoscopic imaging techniques: beyond narrow band. *Am J Gastroenterol* 2018; 113: 1103–1107
- [7] Cronin J, McAdam E, Danikas A et al. Epidermal growth factor receptor (EGFR) is overexpressed in high-grade dysplasia and adenocarcinoma of the esophagus and may represent a biomarker of histological progression in Barrett's esophagus (BE). *Am J Gastroenterol* 2011; 106: 46–56
- [8] Plum PS, Gebauer F, Krämer M et al. HER2/neu (ERBB2) expression and gene amplification correlates with better survival in esophageal adenocarcinoma. *BMC Cancer* 2019; 19: 38
- [9] Zhou J, Joshi BP, Duan X et al. EGFR overexpressed in colonic neoplasia can be detected on wide-field endoscopic imaging. *Clin Transl Gastroenterol* 2015; 6: e101
- [10] Joshi BP, Zhou J, Pant A et al. Design and synthesis of near-infrared peptide for in vivo molecular imaging of HER2. *Bioconjug Chem* 2016; 27: 481–494
- [11] Chen J, Zhou J, Gao Z et al. Multiplexed targeting of Barrett's neoplasia with a heterobivalent ligand: Imaging study on mouse xenograft in vivo and human specimens ex vivo. *J Med Chem* 2018; 61: 5323–5331
- [12] Chen J, Gao Z, Li G et al. Dual-modal in vivo fluorescence and photoacoustic imaging using a heterodimeric peptide. *Chem Comm* 2018; 54: 13196–13199
- [13] Chen J, Jiang Y, Chang TS et al. Multiplexed endoscopic imaging of Barrett's neoplasia using targeted fluorescent heptapeptides in a phase 1 proof-of-concept study. *Gut* 2021; 70: 1010–1013
- [14] Bird-Lieberman EL, Neves AA, Lao-Sirieix P et al. Molecular imaging using fluorescent lectins permits rapid endoscopic identification of dysplasia in Barrett's esophagus. *Nat Med* 2012; 18: 315–321
- [15] Nagengast WB, Hartmans E, Garcia-Allende PB et al. Near-infrared fluorescence molecular endoscopy detects dysplastic oesophageal lesions using topical and systemic tracer of vascular endothelial growth factor A. *Gut* 2019; 68: 7–10
- [16] Labrijn AF, Janmaat ML, Reichert JM et al. Bispecific antibodies: a mechanistic review of the pipeline. *Nat Rev Drug Discov* 2019; 18: 585–608
- [17] Ding L, Tian C, Feng S et al. Small sized EGFR1 and HER2 specific bifunctional antibody for targeted cancer therapy. *Theranostics* 2015; 5: 378
- [18] Yan Y, Chen X. Peptide heterodimers for molecular imaging. *Amino Acids* 2011; 41: 1081–1092
- [19] Zhang J, Niu G, Lang L et al. Clinical translation of a dual integrin $\alpha_v\beta_3$ - and gastrin-releasing peptide receptor-targeting PET radiotracer, ^{68}Ga -BBN-RGD. *J Nucl Med* 2017; 58: 228–234
- [20] Razumienko EJ, Chen JC, Cai Z et al. Dual-receptor-targeted radioimmunotherapy of human breast cancer xenografts in athymic mice coexpressing HER2 and EGFR using ^{177}Lu - or ^{111}In -labeled bispecific radioimmunoconjugates. *J Nucl Med* 2016; 57: 444–452